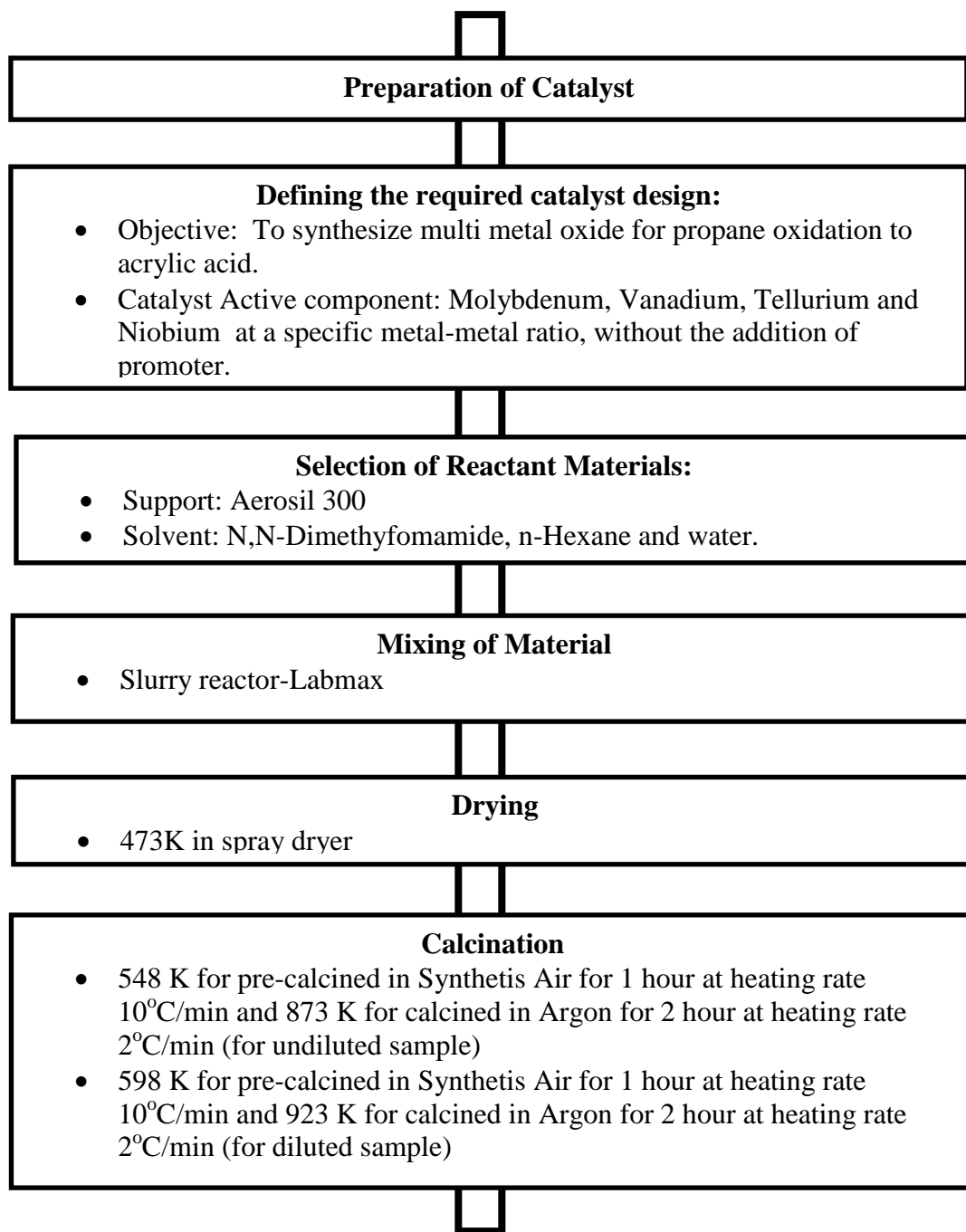


3.0 Methodology

In this chapter, details on the materials, gases, methodology of catalyst synthesis and its subsequent activation, catalytic performance and product analysis are discussed. In addition, the promising catalysts are further characterized using a variety of analytical techniques.

Preparation of catalyst involves several main steps (Scheme 3.1):

- (a) Identifying the required catalyst design for a defined process; judgment of reactivity pattern of the catalyst metals based on past experience and understanding of the desired reaction mechanisms and kinetics
- (b) Selection of the required reactant materials (support, precursors of the active components and promoters and water or solvent).
- (c) Preparation of catalyst precursor by LabMax
- (d) Drying catalyst precursor by spray dryer.
- (e) Calcination (the desired crystalline structure, maximum temperature, the rate of heating and atmosphere)
- (f) Catalytic performance of catalyst (screening using high throughput Nanoflow).



Scheme 3.1: Overview of Synthesis and Testing Work Flow.

3.1 Materials and Gases

3.1.1 List of material and gases used

Table 3.1: List of chemicals used

| Chemicals | Brand | Formula molecule | Molecular weight, (g/mol) | Purity (%) |
|---------------------------------------|----------------|--|---------------------------|---------------------------------|
| Ammonium molybdate tetrahydrate (AHM) | Merck | $(\text{NH}_4)_6\text{Mo}_7\text{O}_{24}\cdot 4\text{H}_2\text{O}$ | 1235.86 | Assay as MoO_3 , 81-83 |
| Ammonium metavanadate (AMV) | Riedel de Häen | NH_4VO_3 | 116.98 | Assay ≥ 99 |
| Telluric acid | Aldrich | $\text{Te}(\text{OH})_6$ | 229.64 | - |
| Ammonium Niobium oxalate | Aldrich | $\text{C}_{10}\text{H}_8\text{N}_2\text{O}_{33}\text{Nb}_2$ | 869.82 | 99.99 |
| N,N Dimethylformamide (DMF) | Aldrich | | | Assay ≥ 99 |
| n-Hexane | Merck | $\text{CH}_3(\text{CH}_2)_4\text{CH}_3$ | 86.18 | 99.0 |

Table 3.2: List of supports used

| Type of support | Commercial name | Specific surface area ($\text{m}^2\cdot\text{g}^{-1}$) |
|-----------------|-----------------|--|
| Silica | Aerosil 300 | 300 |

Table 3.3: List of gases and purity

| Type of Gas | Brand | Purity (%) |
|---------------|-------|------------|
| Argon | MOX | 99.90 |
| Nitrogen | MOX | 99.99 |
| Oxygen | MOX | 99.50 |
| Synthetic Air | MOX | 99.90 |
| Propane | MOX | 99.80 |

3.2 Preparation of Catalyst Precursor

This chapter explained in detail the important equipment used, the preparation of the catalysts precursor and the activation step in order to develop an active catalyst for selective oxidation of propane to acrylic acid.

3.2.1 LabMax (Stock Solution Workstation)

The METTLER TOLEDO LabMax® is a fully automated lab reactor which is used to perform chemical reactions (Figure 3.1). With this reactor new method for preparative chemistry can be quickly developed and optimized. The WinRC software allows the LabMax to be controlled by a computer.

The LabMax is different from other conventional analytical lab instruments in that a chemical hazard potential can arise with investigations on a liter scale. It has therefore been professionally designed in accordance with state-of-the-art technology with regard to safety and product quality.

The LabMax system comprises with glass stirrer, chemical reactor and a PC. The instruments form a single unit for performing experiments; the PC can be used as a single unit for pre-programming an experiment and for evaluating experimental data. The LabMax comprises 3 modules including the thermostating unit, the controller unit and the thermostat. The modules are assembled mechanically to form a single unit. Both control units are housed in the electronics cabinet, which can be purged with an inert gas; the thermostat has its own housing. The reactor in which the chemical reaction under investigation conducted is attached to the thermostat housing.

There are several parameters that must be set before beginning an experiment. First, the initial temperature and stirrer speed must be set. Secondly, safety parameters must be defined. These are given in values, that when exceeded, will cause LabMax to trigger an emergency program. Thirdly, a defined standard operating procedure (SOP) must be set. A SOP is represented by many stages. Each stage is composed of a specific time length, temperature, and stirrer speed. Once the experiment is completed, the solutions are injected from the valve into the glass reactor tank for reactions. In order to minimize the aging time of the resulting precipitates, the slurry was spray dried directly from the reactor. The dried precursor then was further underwent heat treatment to obtain the active catalyst



Figure 3.1: LabMax Reactor

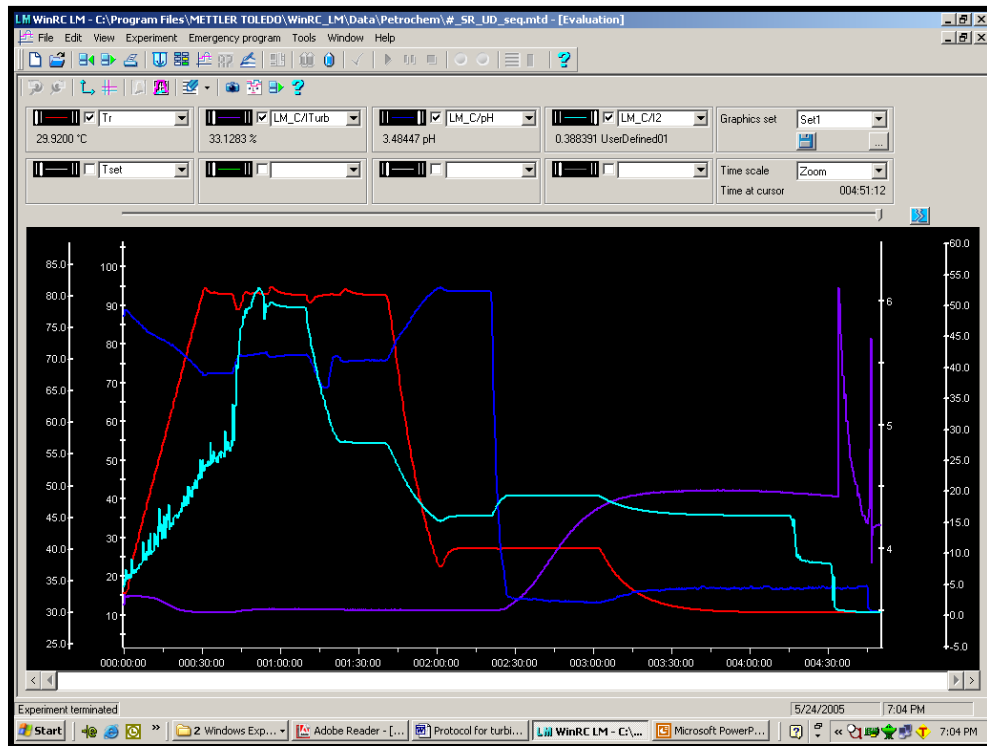


Figure 3.2: In-situ profiles obtained from LabMax experiment

Figure 3.2 shows the in-situ profile diagram monitored from LabMax reactor system. Every axis shown in the profile diagram indicated different parameters that measured during the reaction. The parameters comprises of **t**emperature (Axis 1), turbidity (%) (Axis 2) , pH (Axis 3) and conductivity (uS/m) (Axis 4). These parameters will be discussed in detailed in section 3.3.

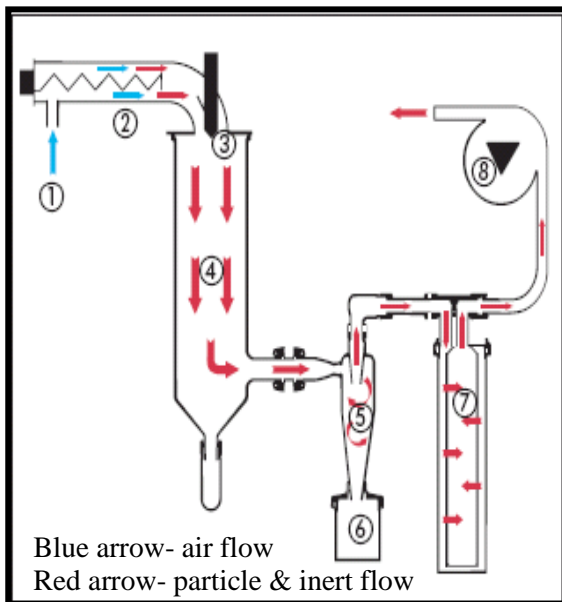
3.2.2 Drying Stock Solution (Büchi Mini Spray Dryer B-290)

Spray drying is a widely applied method used in drying aqueous solutions, organic solutions, and emulsions. Dry milk powder, detergents and dyes are the examples of spray dried products which are currently available in the market. Spray drying is a quick drying method used in preserving foods. The spray dried process occurs when the feed from a fluid state is passed into a hot drying medium and finally a dried particulate can be formed. Intensive research and development during the last two decades has resulted in spray drying becoming a highly competitive means of drying a wide variety of products. The range of product applications continues to expand, so that today spray drying has connections with many things we use daily.

Spray drying involves the evaporation of moisture from an atomized feed by mixing the spray and the drying medium. The drying medium is typically air. The drying proceeds until the desired moisture content is reached in the sprayed particles and the product is then separated from the air. The mixture being sprayed can be a solvent, emulsion, suspension or dispersion. In this study, Büchi Mini Spray Dryer B-290 was used as pictured in Figure 3.3. The principle of the drying air and feed shown in Figure 3.4 and Figure 3.5



Figure 3.3: Spray Dryer Büchi spray dryer B-290



Functional principle of the drying air

The Mini Spray Dryer B-290 operates according to a co-current air and product stream. This means that sprayed product and hot air have the same flow direction.

- 1_ Air inlet
- 2_ Electric heater
- 3_ Concentric inlet of the hot air around the spray nozzle
- 4_ Spray Cylinder
- 5_ Cyclone to separate particles from gas stream
- 6_ Collecting vessel for dried product
- 7_ Outlet filter
- 8_ Aspirator to pump air through System

Figure 3.4: Functional principle of the drying air

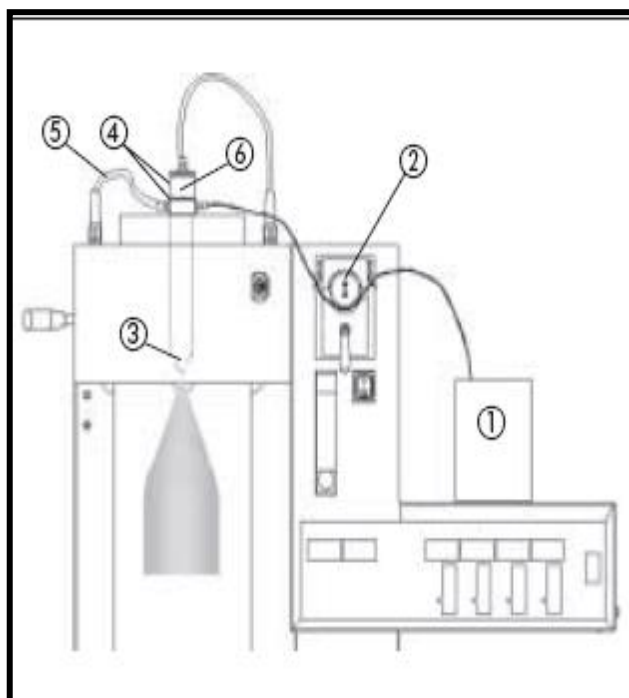


Figure 3.5: Functional principle of the feed and dispersion

Functional Principle of the sample feed and dispersion

The Mini Spray Dryer has a integrated two-fluid nozzle:

Compressed air is used to disperse the liquid body into fine droplets which are subsequently dried in the cylinder.

- 1_ Feed solution
- 2_ Peristaltic pump
- 3_ Two fluid nozzle
- 4_ Connection for cooling water
- 5_ Connection for compressed air
- 6_ Automatic nozzle cleaning system

[refer as Manual of BÜCHI Spray Dryer B-290]

Thus, the instrument settings, namely inlet temperature, feed rate, spray air flow and aspirator flow are in a combined system influencing the product parameters: Temperature load, Final humidity, Particle size and Yield. The optimisation of these parameters is usually made in a “Trial & Error” process. Some initial conditions can be found in the application database for equal or similar products.

Table 3.4: Some initial conditions that can be followed for other similar products

| parameter \ dependence | aspirator rate ↑ | air humidity ↑ | inlet temperature ↑ | spray air flow ↑ | feed rate ↑ | solvent instead of water | concentration ↑ |
|---------------------------|--|--|---|--------------------------------------|--|--|---|
| outlet temperature | ↑↑ less heat losses based on total inlet of energy | ↑ more energy stored in humidity | ↑↑↑ direct proportion | ↓ more cool air to be heated up | ↓↓ more solvent to be evaporated | ↑↑↑ less heat of energy of solvent | ↑↑ less water to be evaporated |
| particle size | - | - | - | ↓↓↓ more energy for fluid dispersion | (↑) more fluid to disperse | (↓) less surface tension | ↑↑↑ more remaining product |
| final humidity of product | ↑↑ lower partial pressure of evaporated water | ↑↑ higher partial pressure of drying air | ↓↓ lower relative humidity in air | - | ↑↑ more water leads to higher partial pressure | ↓↓↓ no water in feed leads to very dry product | ↓ less water evaporated, lower partial pressure |
| yield | ↑↑ better separation rate in cyclone | (↓) more humidity can lead to sticking product | (↑) eventually dryer product prevent sticking | - | (↓↑) depends on application | ↑↑ no hygroscopic behaviour leads to easier drying | ↑ bigger particles lead to higher separation |

Below explained the interaction of the individual parameters:

- Higher temperature differences between the inlet and outlet temperatures result in a higher amount of residual moisture.
- A high aspirator speed means a shorter residence time in the device and results in a larger amount of residual moisture.
- A high aspirator speed results in a higher degree of separation in the cyclone.
- Higher spray flow rates tend to result in smaller particles.
- Higher spray concentrations result in larger particles.
- Higher pump speed, result in a lower outlet temperature. (BÜCHI 1997-2002)

3.3 Preparation method and conditions for the $\text{Mo}_1\text{V}_{0.3}\text{Te}_{0.23}\text{Nb}_{0.125}\text{O}_x$ catalyst

3.3.1 The Undiluted MoVTe(Nb) Catalysts

The method of catalyst preparation consists of different stages, including the preparation of watery precursor solution, the drying process via spray drying and the final step which involves the calcination of dry precursor powders to the “fresh” catalyst. The current preparation routine for $\text{Mo}_1\text{V}_{0.30}\text{Te}_{0.23}\text{Nb}_{0.125}\text{O}_x$ is based on a patent by Rohm and Haas in 1999 (Lin 1999).

3.3.1.1 Preparation of precursor without addition of oxalic acid (standard recipe)

$\text{Mo}_1\text{V}_{0.30}\text{Te}_{0.23}\text{Nb}_{0.125}\text{O}_x$ has been obtained using the method described in the patent literature (Lin 1999). Preparation of slurry containing metal elements of Mo, V, Te and Nb, was according to the following procedure: 112.65 g of ammonium heptamolybdate tetrahydrate (AHM) from Merck was dissolved in about 500ml of deionized water. The mixture solution was heated up to temperature 353 K under constant stirring, followed by the addition 22.45 g of ammonium metavanadate (AMV) from Riedel de Häen. Then, 33.70 g of Telluric acid powder (Aldrich) was added to the solution under stirring to obtain MoVTe solution. Afterwards, the MoVTe solution was cooled down to 313 K. Finally, an aqueous solution of Niobium oxalate 35.2 g in 145 ml of deionized water was slowly added. The obtained slurry was stirred vigorously for about 30 minutes before being introduced to the drying technique which is Spray Drying. The catalyst precursor synthesis was carried out using LabMax reactor (Mettler Toledo) as shown in Figure 3.6 . The nominal metal ratio of these catalyst formed from this slurry is $\text{Mo}_1\text{V}_{0.3}\text{Te}_{0.23}\text{Nb}_{0.125}$. This procedure is illustrated in Scheme 3.2 where a detailed description of the typical

preparation methods and conditions used is included, followed by a preferred preparation procedure.

3.3.1.2 Preparation of precursor with addition of oxalic acid

The typical preparation to obtain an aqueous precursors-slurry is as follows. In a Labmax reactor, 1285 g of deionised water and 78.63 g of AHM were sequentially dissolved upon heating to about 353 K. Then, 15.63 g of AMV was added into the solution and followed by 23.52 g of Telluric acid. This solution was cooled at about 313 K. Then mixture of 25.60 g of niobium oxalate and 8.90 g of oxalic acid were dissolved into 359 g of deionised water in room temperature (303 K). This solution was added into the LabMax reactor to obtain the slurry. The slurry was stirred vigorously for 30 minutes before transferred into a spray dried. About 100 g of orange fine product were collected upon spray drying. Spray dryer operating conditions are described in Section 3.3.

3.3.2 The Diluted MoVTe(Nb) Catalysts

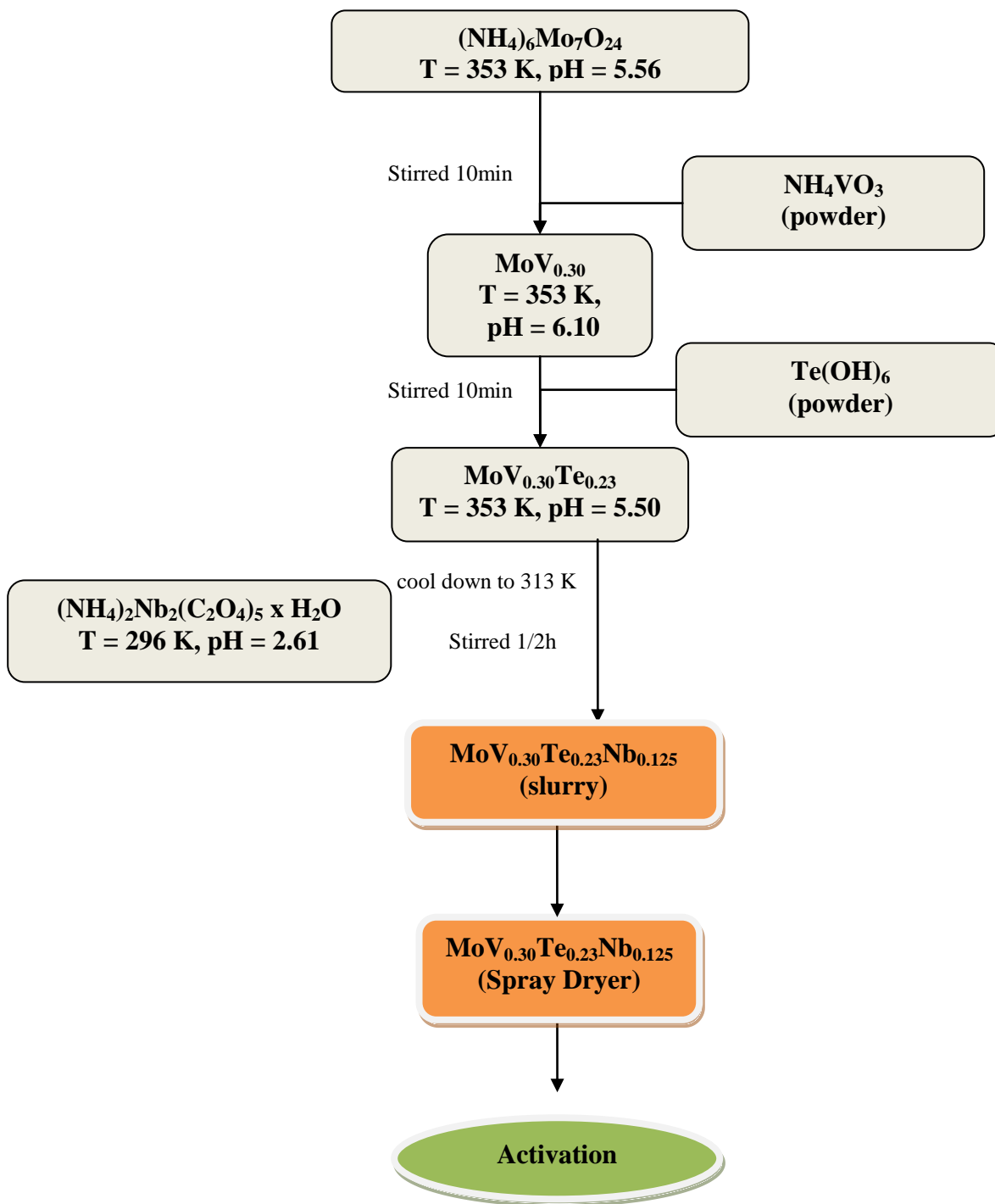
3.3.2.1 Preparation of precursor without addition of oxalic acid

The procedure in preparing the diluted system is similar to the case as in the undiluted system. The difference is that the support is added during the catalyst preparation. A slurry containing all elements, Mo, V, Te was prepared first according to the following procedure in LabMax reactor: 112.72 g of AHM, 22.4 g of AMV and 33.7 g of Telluric acid was sequentially dissolved in 1000 ml of deionised water at 353 K. Then, the solution was cooled down to 313 K. The support (Aerosil 300) was added and stirred for 10 min. Finally, aqueous solution of 35.3 g of ammonium niobium oxalate was slowly added to the solution

and stirred for 1 h until orange slurry obtained. After 1 h of stirring, the slurry was introduced into a Büchi B290 spray dryer.

3.3.2.2 Preparation of precursor with addition of oxalic acid

$\text{Mo}_1\text{V}_{0.30}\text{Te}_{0.23}\text{Nb}_{0.125}\text{O}_x$ was prepared according to the method mentioned in the patent literature. Two solutions were prepared, the first one containing 78.86 g of AHM, 15.64 g of AMV and 23.54 g of telluric acid was sequentially dissolved in 1286 g of deionised water at 353 K. The second solution was prepared by dissolving 25.62 g of ammonium niobium oxalate in 360 g deionised water without heating. Before second solution is slowly added into first solution, 100 g of Aerosil 300 was added and stirred for 10 min followed by the addition of second solution. The solution mixture was stirred for 1 h before spray dried.



Scheme 3.2: Preparation steps for MoVTeNbO_x sample (As a standard catalyst)

3.4 Spray Drying Method

The slurry (gel) that obtained from the LabMax reactor was brought into the next step which is drying stage. A Büchi spray dryer B-291 was used to dry the slurry taken from LabMax reactor. The purpose of drying is to remove the solvent from the precursor solution or slurry. Normally, it is the second step of the metal-oxides preparation. The spray drying condition was mentioned in the table below (Table 3.5):

Table 3.5: Spray dryer operating conditions

| Operating Condition | Reading |
|---------------------|---------|
| Inlet Pressure | 5 bar |
| Inlet Temperature | 473 K |
| Outlet Temperature | 376 K |
| Aspirator | 100% |
| Pump | 30% |



Figure 3.6: LabMax

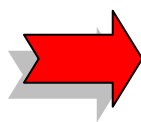


Figure 3.7: Spray Dryer

3.5 Catalyst Activation

The spray-dried material was calcined in URN which is placed inside Carbolite CWF 1200 furnace (**Figure 3.8**) at 548 K for undiluted system and 598 K for diluted system under air with heating rate of 10 K/min and hold for 1 hour. Synthetic air was purged for 30 minutes before the ramping started. After cooling to 303 K, it was subsequently treated in flowing Argon at 873 K for undiluted system and 923 K for diluted system with heating rate of 2 K/min and for hold for another two hours in which these results in black fine powder formation. For undiluted system, the final catalyst is 67.8 %wt Mo-V-Te-Nb (metals) (100%wt Mo-V-Te-Nb metal oxides). While for diluted system, the final catalyst comprised 33.9 %wt Mo-V-Te-Nb (metals) (50% wt Mo-V-Te-Nb metal oxides).

In the process of the present application, the materials that had been calcined according to the calcination steps were known as metal oxide catalyst comprising oxides of Mo, V, Te and Nb. These oxide catalysts were transferred to the high-throughput reactor for screening processes. The details on the reaction conditions will be discussed in Section 3.8. From the screening results, catalysts from one of the drying techniques were selected to undergo leaching process and also a few other characterization techniques to investigate the properties of the catalyst.

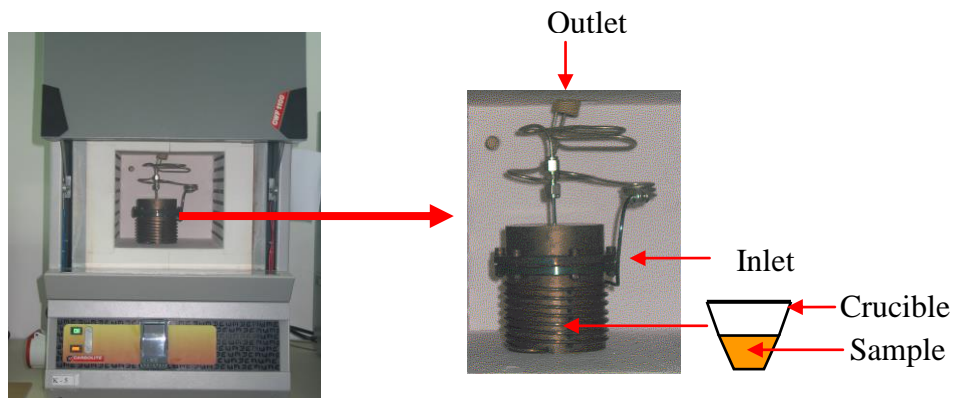


Figure 3.8: The urn reactor for calcinations of precursor sample

3.6 Surface Modification on MoVTeNb Oxide Catalyst

- (i) The undiluted $\text{Mo}_1\text{-V}_{0.3}\text{-Te}_{0.23}\text{-Nb}_{0.125}\text{-O}_x$ leached in different solvents i.e; water, ammonia and nitric acid for 1 hour.**

1 g of activated material was dispersed in 100mL of distilled water at 300 K for 1 hour. The sample was centrifuged for 20 min, and the remaining solid was dried in vacuum desiccators. The experiments were repeated for different solvents i.e. 0.1M of nitric acid and 0.1 M of ammonia.

- (ii) The undiluted $\text{Mo}_1\text{-V}_{0.3}\text{-Te}_{0.23}\text{-Nb}_{0.125}\text{-O}_x$ leached in water at different times.**

10 g dried and activated material was dispersed in 1000mL of distilled water at 300 K. 50 ml of the sample was taken out by a pipette at 5 min (619), 1 h (621), 24 h (624) and after 80 h (680). The samples were centrifuged for 20 min, and the remaining solids were dried in the vacuum desiccators.

(iii) The undiluted and diluted $\text{Mo}_1\text{-V}_{0.3}\text{-Te}_{0.23}\text{-Nb}_{0.125}\text{-O}_x$, catalysts leached in water for 1 hr.

1 g activated material was leached in 100mL of distilled water for 1 h. The sample was centrifuged for 20 min and dried in vacuum desiccators. The experiment was repeated for diluted MoVTeNb oxide catalyst.

(iv) The undiluted and diluted $\text{Mo}_1\text{-V}_{0.3}\text{-Te}_{0.23}\text{-Nb}_{0.125}\text{-O}_x$, catalysts leached in water for 24 hr.

Repeating the procedure above, 1 g activated material was leached in 100mL of distilled water for 1 h. The sample was centrifuged for 20 min and dried in vacuum desiccators. This procedure also applied for diluted MoVTeNb oxide catalyst.

3.7 Catalyst Characterization

3.7.1 Powder X-Ray Diffraction (XRD) Analysis

Powder X-Ray Diffraction (PXRD) is one of the most frequently applied techniques in catalyst characterization. X-ray with wavelengths in the Å range, is sufficiently energetic in penetrating the solid and are well suited to probe their internal structure. XRD is therefore used to identify bulk crystalline phases and to estimate particle sizes (Cohen J.B. 1997).

X-rays were discovered by W.C. Röntgen in 1895, and led to three major uses:

- X-ray radiography is used for creating images of light-opaque materials relies on the relationship between density of materials and absorption of x-rays. Applications include a variety of medical and industrial applications.

- X-ray crystallography relies on the dual wave/particle nature of x-rays to discover information about the structure of crystalline materials.
- X-ray fluorescence spectrometry relies on characteristic secondary radiation emitted by materials when excited by a high-energy x-ray source and is used primarily to determine the amounts of particular elements in materials.

The powder diffraction method, ~~by~~ using conventional X-ray sources, was devised independently in 1916 by Debye and Scherrer in Germany and in 1917 by Hull in the United States. The technique developed steadily and, half a century later, the ‘traditional’ applications, such as phase identification, the determination of accurate unit-cell dimensions and the analysis of structural imperfections, were well established. Powder data have been used for the identification of unknown materials or mixtures of phases since the late 1930s. Phase identification sometimes precedes athe quantitative analysis of compounds present in a sample and powder diffraction is frequently the only approach ~~available to the analyst~~ for this purpose. A new development in quantitative analysis is the use of the Rietveld method with multi-phase refinement. The physics and mathematics describing the generation of monochromatic X-rays, and the diffraction of those X-rays by crystalline powders are very complex. Below in Figure 3.109, it showed the schematic diagram of a diffractometers system for the XRD.

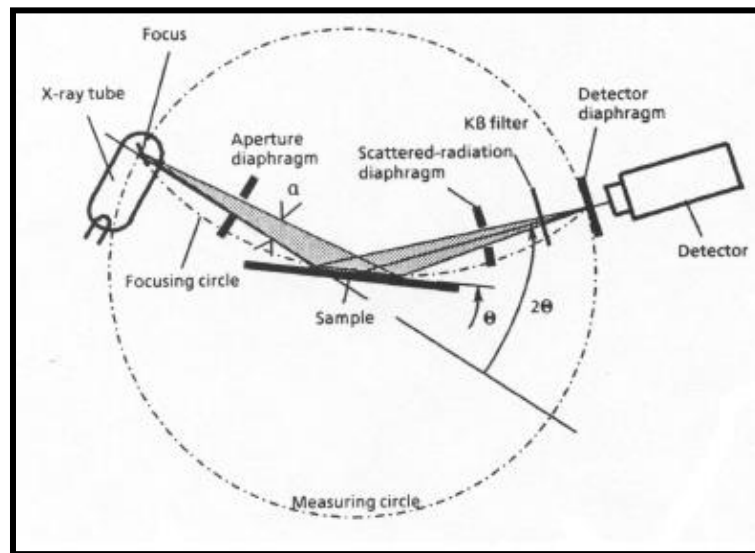


Figure 3.109: Schematic diagram for a diffractometers system

An x-ray source consists of a X-ray tube and beams, which is bombarded to the electrons. The emitted x-rays arise from two processes. Electron slow down by the target emits a continuous background spectrum of Bremsstrahlung or braking radiation. Superimposed on this are characteristic narrow lines. The Cu K_α line arises when primary electron creates a core hole in the K shell, which is filled by an electron from the L shell (K_β : the K-hole is filled from the M-shell electron, etc) under emission of an x-ray quantum (Sahar 1993).

Different features of powder diffraction pattern can be exploited in the characterization of material. XRD data are mostly used as a “fingerprint” in the identification of materials (Table 3.26).

Table 3.6: Details ~~information in the powder of powder~~ X-ray diffraction (XRD).

| Feature | Information |
|----------------------------------|------------------------------------|
| Peak position (2θ value) | Unit Cell Dimension |
| Non-indexable Line | Presence of Crystalline impurities |
| Background | Presence of amorphous material |
| Width of Peak | Crystalline Size |
| Peak Intensities | Crystal Structure |

The diffraction line for a powder sample occurs because ~~of~~ a small fraction of particles are oriented in such a way that by chance a certain crystal plane (hkl) is at the right angle with the incident beams for constructive interferences. Diffraction lines from perfect crystals are very narrow, whereas, crystalline size below 100nm causes broadening due to incomplete destructive interference in scattering directions where the x-ray is out of phase. d_{hkl} for a relatively big crystal can be obtained by using Bragg's law and assuming first order diffraction:

$$\lambda = 2d_{hkl} \sin \theta; \text{ with } \lambda = 0.1542 \text{ (for Cu } K_{\alpha} \text{) radiation}$$

If the crystalline is very small (<50nm), then Bragg condition is no longer satisfied, and the residual scattered intensity will be detected ~~at~~ angles away from the Bragg angle. As a

consequence, the reflection broadens (as mentioned above). The broadening is related to the average crystallite size by Scherrer equation:

$$D = k\lambda / \beta \cos \theta$$

With k constant 0.9, $\lambda = 0.1542$ (for Cu $K\alpha$) radiation, and β = true line width

$$\beta = (B^2 - b^2)^{1/2}$$

With B = measured line width, and b = instrumental broadening of diffractometer.

XRD ~~is an~~ involves the elastic scattering of x-ray photons by atoms in a periodic lattice.

The scattered monochromatic x-rays that are in phase give constructive interference. The

XRD pattern of a powdered sample is measured with a stationary x-ray source (usually Cu

$K\alpha$) and a movable detector, which scans the intensity of the diffracted beams. The width

of diffraction peaks carries information on the dimensions of the reflecting planes.

Diffraction lines from perfect crystals are very narrow (Langford J.I. 1996). For crystallite

sizes below 100nm, however line broadening occurs due to incomplete destructive

interference in scattering directions where the x-ray is out

of phase.



Figure 3.140: D8 Bruker X-Ray Diffractometer

Principle of Operation

To identify the crystal lattice dimensions, structure and composition of material, XRD was performed using a Bruker X-ray Diffractometer model D-8 equipped with EVA Diffract software for data acquisition and analysis. Data were acquired using a CuK_α monochromatized radiation source operated at 40 kV and 40 mA at ambient temperature. About on 200-500 mg of powdered samples were finely grounded and placed in the Si single crystal sample holder, with the powder lightly pressed into place using a microscopic slide. The surface of the sample was flattened and smoothened.

The sample holder was then placed in the diffractometer stage with continuous rotation throughout exposure for analysis. A continuous 2θ scan mode from 2° - 80° was used for high degree scanning at step time of 15 s and step size of $0.02^{\circ}\text{s}^{-1}$. A divergence slit was inserted to ensure that the x-rays focused only on the sample, and not the edges of specimen holder. Diffractogram generation and analysis were done by Bruker EVA version 8.02 and compare with standard crystalline reference from International Crystal Diffraction Database (ICDD). The diffractograms obtained were matched against the Joint Committee on Powder Diffraction Standards (JCPDS) PDF 1 database version 2.6 to confirm the precursor and catalyst phase.

3.7.2 X-Ray Fluorescence

X-Ray Fluorescence is a spectroscopic technique of analysis based on the fluorescence of atom in X-ray domain, to provide qualitative and quantitative information on the elemental composition of a sample. Excitation of the atom is achieved by an X-ray beam or by bombardment with particles such as electrons. The universality of this phenomenon, the speed which the measurement can be obtained and the potential to examine most materials without preparation all contribute to the success of this analytical method, which does not destroy the sample. However, the calibration procedure for XRF is a delicate operation.

This technique is a fast, non-destructive and environmentally friendly analysis method with very high accuracy and reproducibility. All elements of the periodic table from beryllium to californium can be measured qualitatively, semi-quantitatively and quantitatively in powders, solids and liquids. Concentrations ~~of~~ up to 100% are analyzed directly, without any dilution, with reproducibility better than $\pm 0.1\%$. Typical limits of detection are from 0.1 to 10 ppm. Most modern X-ray spectrometers with modular sample changers enable fast, flexible sample handling and adaptation to customer-specific automation processes.

XRF samples ~~can be solids~~are solids such as glass, ceramic, metal, rock, coal, or plastic. They can also be liquids, like petrol, oil, paint, solutions, blood or even wine. Petroleum ~~I~~industry, geology, paper mills, toxicology and environmental applications (dust, fumes from combustion, heavy metals and dangerous materials in waste such as Pb, As, Cr, Cd, etc.) are included as well. With an XRF spectrometer both very small concentrations of very few ppm and very high concentrations of up to 100% can be analyzed directly without any dilution process.

Based on its simple and fast sample preparation requirements, XRF analysis is a universal analysis ~~method, method which has been~~ widely accepted in the fields of research and industrial process control. XRF is particularly effective for complex environmental analysis and for production and quality control of intermediate and end products. The quality of sample preparation for XRF analysis is ~~at least~~ as important as the quality of measurements.

An ideal sample is prepared so that it is:

- ◆ representative of the material
- ◆ homogeneous
- ◆ thick enough to meet the requirements of an infinitely thick sample
- ◆ without surface irregularities
- ◆ composed of small enough particles for the wavelengths to be measured

With XRF it is not necessary to bring solid samples into solution and be burdened with chemical disposal procedures, then dispose of solution residues, as is the case with all wet-chemical methods. The main prerequisite for exact and reproducible analysis is a plain, homogeneous and clean analysis surface. For analysis of very light elements, e.g. beryllium, boron and carbon, the fluorescence radiation to be analyzed originates from a layer whose thickness is only a few atom layers to a few tenths of micrometer and which strongly depends on the sample material (Table 3.37). Careful sample preparation is therefore extremely important for the analysis of light elements.

Table 3.7: Layer thickness (h, in μm), from which 90% of the fluorescence radiation originates

| Sample matrix | | Graphite | Glass | Iron | Lead |
|---------------|-------------|---------------------------|---------------------------|---------------------------|---------------------------|
| Line | | $h_{(90\%, \mu\text{m})}$ | $h_{(90\%, \mu\text{m})}$ | $h_{(90\%, \mu\text{m})}$ | $h_{(90\%, \mu\text{m})}$ |
| U | $L\alpha_1$ | 28000 | 1735 | 154 | 22.4 |
| Pb | $L\beta_1$ | 22200 | 1398 | 125 | 63.9 |
| Hg | $L\alpha_1$ | 10750 | 709 | 65.6 | 34.9 |
| W | $L\alpha_1$ | 6289 | 429 | 40.9 | 22.4 |
| Ce | $L\beta_1$ | 1484 | 113 | 96.1 | 6.72 |

| | | | | | |
|-----------------------------|---|---|---|---|--------------------|
| Ba | $L\alpha_1$ | 893 | 71.3 | 61.3 | 4.4 |
| Sn | $L\alpha_1$ | 399 | 44.8 | 30.2 | 3.34 |
| Cd | $K\alpha_1$ | 144600 | 8197 | 701 | 77.3 |
| Mo | $K\alpha_1$ | 60580 | 3600 | 314 | 36.7 |
| Zr | $K\alpha_1$ | 44130 | 2668 | 235 | 28.9 |
| Sr | $K\alpha_1$ | 31620 | 1947 | 173 | 24.6 |
| Br | $K\alpha_{1,2}$ | 18580 | 1183 | 106 | 55.1 |
| As | $K\beta_1$ | 17773 | 1132 | 102 | 53 |
| Zn | $K\alpha_{1,2}$ | 6861 | 466 | 44.1 | 24 |
| Cu | $K\alpha_{1,2}$ | 5512 | 380 | 36.4 | 20 |
| Ni | $K\alpha_{1,2}$ | 4394 | 307 | 29.8 | 16.6 |
| Fe | $K\alpha_{1,2}$ | 2720 | 196 | 164 | 11.1 |
| Mn | $K\alpha_{1,2}$ | 2110 | 155 | 131 | 9.01 |
| Cr | $K\alpha_{1,2}$ | 1619 | 122 | 104 | 7.23 |
| <u>Sample matrix</u> | | <u>Graphite</u> | <u>Glass</u> | <u>Iron</u> | <u>Lead</u> |
| <u>Line</u> | <u>h (90%, μm)</u> | <u>h (90%, μm)</u> | <u>h (90%, μm)</u> | <u>h (90%, μm)</u> | <u>Line</u> |
| Ti | $K\alpha_{1,2}$ | 920 | 73.3 | 63 | 4.52 |
| Ca | $K\alpha_{1,2}$ | 495 | 54.3 | 36.5 | 3.41 |
| K | $K\alpha_{1,2}$ | 355 | 40.2 | 27.2 | 3.04 |
| Cl | $K\alpha_{1,2}$ | 172 | 20.9 | 14.3 | 2.19 |
| S | $K\alpha_{1,2}$ | 116 | 14.8 | 10.1 | 4.83 |
| Si | $K\alpha_{1,2}$ | 48.9 | 16.1 | 4.69 | 2.47 |
| Al | $K\alpha_{1,2}$ | 31.8 | 10.5 | 3.05 | 1.7 |

| | | | | | |
|----|-----------------|-------|-------|---------|---------|
| Mg | $K\alpha_{1,2}$ | 20 | 7.08 | 1.92 | 1.13 |
| Na | $K\alpha_{1,2}$ | 12 | 5.56 | 1.15 | 0.728 |
| F | $K\alpha_{1,2}$ | 3.7 | 1.71 | 0.356 | 0.262 |
| O | $K\alpha_{1,2}$ | 1.85 | 2.50 | 0.178 | 0.143 |
| N | $K\alpha_{1,2}$ | 0.831 | 1.11 | 0.08018 | 0.07133 |
| C | $K\alpha_{1,2}$ | 13.6 | 0.424 | 0.03108 | 0.03124 |
| B | $K\alpha_{1,2}$ | 4.19 | 0.134 | 0.01002 | 0.01166 |

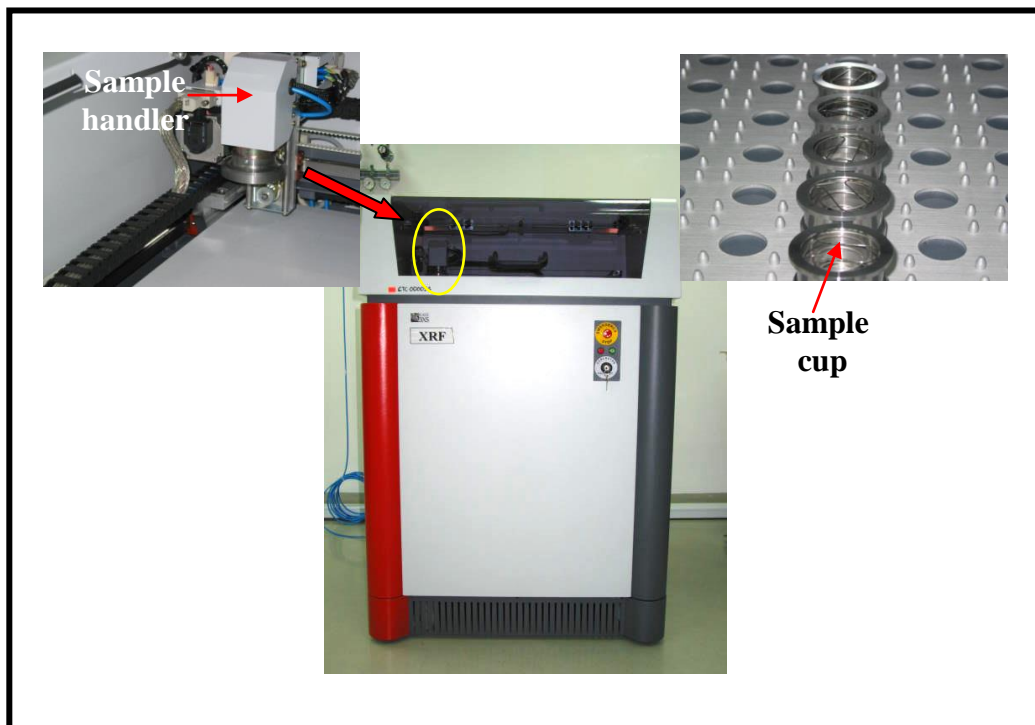


Figure 3.121: X-Ray Florescence S4 EXPLORER

Principle of Operation

In order to use SEM/EDX as a tool for elemental composition, XRF can be another solution to perform elemental composition ~~in~~for all kinds of samples. XRF combines ~~the~~ highest accuracy and precision with simple and fast sample preparation for the analysis of elements from Beryllium (Be) to Uranium (U) in the concentration range from 100 % down to ~~the~~ sub-ppm-level. The measurement was performed by X-Ray Fluorescence S4 EXPLORER equipped with the SPECTRA^{PLUS} V1.64 software. These XRF is equipped with an improve facilities which are listed below:

- ◆ Ceramic end –window Rh target x-ray tube fitted with 75 µm window and 1000 W power.
- ◆ Ten position programmable primary beam filter changer
- ◆ Crystal changer with four crystals (LiF 220), (LiF 200), PET and synthetic multi-layer for measuring Mg, Na, F and O.
- ◆ Super high transmission sealed proportional counter able to measure elements down to Be.
- ◆ Scintillation counter for analysis of higher energy elements.
- ◆ Robotic sample changer with 60 position magazine.

There are three types of sample preparation that are required on this XRF depending on the sample nature:

1. Preparation of solid samples
2. Preparation of liquid samples
3. Preparation of filter samples

(a) Preparation of solid samples

For solid samples, there are two types of preparation ~~for/or which is~~ metals, pressed pallet or fused beads depending on samples itself. Preparation of metal must be simple, rapid and reproducible. Usually, metal samples are prepared as solid disks by conventional ~~of~~ method machining, cutting, milling and polishing. Grinding is used for hard alloys and brittle materials such as ceramic. The best polishing operation are require very fine abrasive to produce the scratch free surface necessary for most analysis, and mirror-like surface if the sample is to be analysed for light elements.

Another method for solid sample is pressed pallet. Since powders are not affected by particle sizes limitations, the quickest and simplest method of preparation is to press powders directly into pallets of equal density, with or without the use of binder. ~~In general, provided those powder particles are less than 50 mm in diameter, t~~The sample will palletize at 10-30 tone in pressure. ~~Where~~When the self-binding properties of the powder are poor, higher pressure may have to be employed or in extreme cases a binder may have to be

used. It is sometimes necessary to add a binder before pelletizing and the choice of the binding agent must be made with care. The binder must be free from significant contaminant elements, have low absorption, stable under vacuum and irradiation conditions, and it must not introduce significant interelement interferences. ~~Of the~~After trying out a large number of binding agents ~~that have been successfully employed, probably~~ the most useful ones are wax and ethyl cellulose.

Analytical data for longer wavelengths will sometimes be improved if a finely ground powder is compacted at higher pressures (say up to 30 t). A 40-ton press should be therefore considered if light element analysis is required in pressed powder samples. A good quality die set is required to produce good quality pressed powder samples. Powders can be pressed into aluminum cups or steel rings. Alternatively boric acid backing can be used, or free pressing if a binder is used.

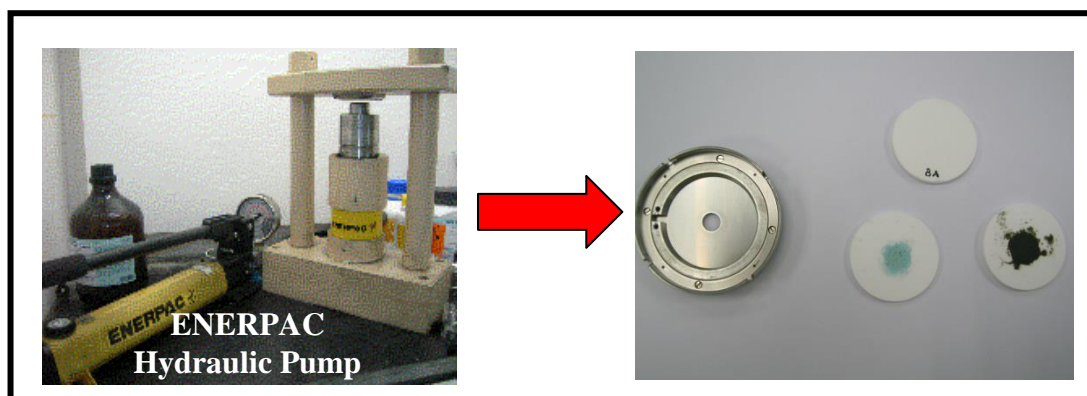


Figure 3.132: Preparation of pressed pellet

The most accurate method for solid sample is fused beading. The dissolution or decomposition of a portion of the sample by a flux and fusion into a homogeneous glass eliminates particle size and mineralogical effects entirely.

The fusion technique also has additional advantages:

- Possibility of high or low specimen dilution for the purpose of decreasing matrix effects
- Possibility of adding compounds such as heavy absorbers or internal standards to decrease or compensate for matrix effects
- Possibility of preparing standards of desired composition

The fusion procedure consists of heating a mixture of sample and flux at high temperatures (800 to 1200 °C) so that the flux melts and the sample dissolves. The overall composition and cooling conditions must be such that the end product ~~after cooling~~ is a one-phase glass after cooling. Heating of the sample-flux mixture is usually done in platinum alloy crucibles, but graphite may also be used when conditions permit. The more frequently used fluxes are borates, namely sodium tetraborate, lithium tetraborate and lithium metaborate. A mixture of these fluxes is sometimes more effective in certain cases. Basically, the ratio between flux and sample is about 75 % (flux) and 25 % (sample).

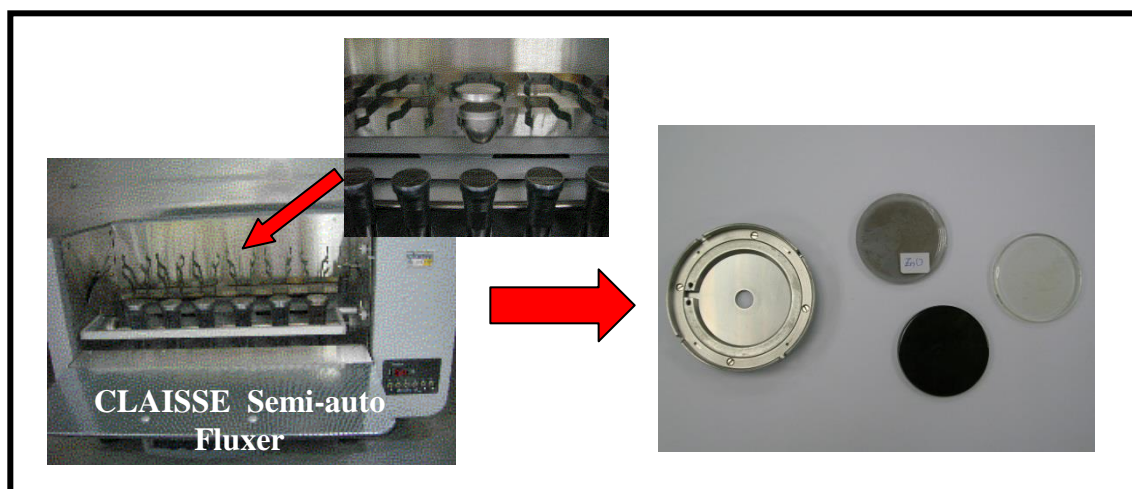


Figure 3.143: Preparation of beads for powder sample

(b) Preparation of liquid or loose powder samples

Provided that the liquid sample to be analyzed is single phase and relatively involatile, it represents an ideal form for presentation to the X-ray spectrometer. A special sample cup (liquid sample holder) and helium path instrument must be used for measurement. The liquid phase is particularly convenient since it offers a very simple means for the preparation of standards and most matrix interferences can be successfully overcome^d by introducing the sample into a liquid solution. Although the majority of matrix interferences can be removed by the solution technique, the process of dealing with a liquid rather than a solid can ~~itself~~ present special problems which, in turn, ~~can~~ limit the usefulness of the technique.

For example, the introduction of a substance into a solution inevitably means a combination of dilution ~~and this, combined with~~ the need for a support window in the sample cell, ~~plus the~~ and the extra background arising from scatter by the low atomic number matrix, invariably leads to a loss of sensitivity, particularly for longer wavelengths (greater than 2.5 Å). Problems can also arise from variations in the thickness and/or composition of the sample support film. The most commonly used types of film are 4 to 6 mm Spectrolene and 2.5 to 6.5 mm Mylar. The liquid samples must be 10-20 ml in constant volume

The process of introducing a sample into a solution can be tedious and difficulties sometimes arise when the ~~where a~~ substance tends to precipitate during analysis. This itself may be due to the limited solubility of the compound or to the photochemical action of the X-rays causing decomposition. In addition, systematic variations in intensity can frequently be traced to the formation of air bubbles on the cell windows following the local heating of the sample. Despite these problems, the liquid solution technique represents a very versatile method of sample handling ~~in that it can remove~~ to remove nearly all matrix effects to the extent that accuracies obtainable with solution methods approach very closely to the ultimate precision of any particular X-ray spectrometer. This method also can ~~apply~~ apply to for loose powder sample.



Figure 3.154: Liquid and loose powder method.

(c) Preparation of filter samples

This technique is required when the concentration of an element in a sample is too low to allow analysis by one of the methods already described, work-up techniques must be used in order to bring the concentration within the detection range of the spectrometer. Concentration methods can be employed where sufficiently large quantities of sample are available. For example, gases, air or water that are contaminated with solid particles can be treated very simply by drawing the gases, air or water through a filter disk followed by direct analysis of the disk in a vacuum environment. Concentration can sometimes be effected simply by evaporating the solution straight onto a confined spot of a filter paper.

This XRF analysis has certain accuracy depending on types of samples preparation that are discussed before. The most accurate method for this analysis is ~~fuse beads~~ fused beading

which is in the range 95 to 100 % accuracy. Then followed by pressed pallets/ solid method around 80 to 90 % and for loose powder/ liquid method is only 70-85 % accuracy.

3.7.3 Scanning Electron Microscopy and Energy Disperseive X-Ray Analysis (SEM/EDX)

Development over past 40 years has resulted in electron microscopes which can **be routinely** to achieve magnifications on the order of one million times and reveal details with a resolution of about 0.1 nm. Electron microscopy is a fairly straightforward technique to determine the size and shape of the catalyst. It also can reveal information on the elemental composition and internal structure of the particles. Two types of electron microscopy that are common used in catalysis *i.e.* transmission electron microscopy (TEM) and scanning electron microscopy (SEM) with EDX. The best way of observing the particle size distribution is by transmission electron microscopy (TEM); since this method can detect particles as small as less than 1 nm. However, the instrumentation is very sophisticated and expensive. Therefore, the next best method available *i.e.* scanning electron microscope with EDX, which **can** reveal details of particles not smaller than 10 nm, was used.

In TEM, a primary electron beam of high energy and high intensity passes through a condenser to produce parallel rays, which impinge on the sample. As the attenuation of the beam depends on the density and the thickness, the transmitted electrons form a two dimensional projection of the sample mass, which is subsequently magnified by the

electron optics to produce a so called bright field image. The dark field image is obtained from the diffracted electrons beams, which are slightly off the angle from the transmitted beam. Typical operating conditions of a TEM instrument are 100-200 keV electrons, 10^{-6} mbar vacuum, 0.5 nm resolution and a magnification of $3 \cdot 10^5$ to 10^6 .

Scanning electron microscopy (SEM) is carried out by rastering a narrow electron beam over the surface and detecting the yield of either secondary or backscattered electrons as function of the position of the primary beam. Contrast is caused by the orientation, parts of the surface facing the detector appearing brighter than parts of the surface with their surface normal pointing away from the detector. The secondary electrons have mostly low energies (in approximately range 5-50 eV) and originate from the surface region of the sample are then collected by a scintillator crystal that converts each electron impact into a flash of light. Each of these light flashes in the crystal is then amplified by a photo multiplier tube and used to build the final image on a fluorescent screen.

The scan of the beam used to form this image is driven in synchrony with that of the electron-exciting beam that scans the specimen, so the resulting image (formed in much the same way as the picture on the television cathode ray tube) is a faithful representation of the specimen surface as imaged by altering size of the area scanned by the scanning beam (FEI 2008).

Energy dispersive analysis of the X-ray radiation is used for qualitative and quantitative compositional information. Corrections for local geometry, self-absorption and the extent

of probe-specimen interaction are required to obtain reliable data. As this is often ignored in analytical data EDX should then be considered as a semi-quantitative method. By moving the electron beam across the material, an image of the spatial distribution of each element in the sample can be acquired (FEI 2008).



Figure 3.165: Scanning Electron Microscope with EDX

Principle of Operation

The precursor or calcined samples were adhered to the aluminium stub using carbon conductive tape. The stub was then mounted on the stub holder and loaded into the chamber. The chamber was evacuated for analysis. Images were recorded with a Quanta 200 FEI microscope instrument and INCA-Suite version 4.02 for EDX analysis. The following settings were used:

Accelerating voltage: HV 5kV (image) and 20 kV (EDX)

Detector type: High vacuum

Working distance: 10 mm

Spot Size: 2.5 – 3

Cone: X-ray

3.7.4 Nitrogen Physisorption Measurement (BET)

Porosity and surface area are important characteristics of solid materials that highly determine the properties and performance of catalysts, sorbents, medicines, rocks, and so on. Physical and chemical gas adsorption as well as mercury intrusion porosimetry are the most widely used techniques to characterize the above-mentioned parameters. The Quantachrome Autosorb Automated Gas Sorption System 6B is based on the static volumetric principle to characterize solid samples by the technique of gas adsorption. It is designed to perform both physisorption and chemisorption enabling determination of the total specific surface area, porosity and the specific surface area of metals present and their dispersion over the surface. Our laboratory can measure specific surface area (SBET), pore volume, pore size distributions in the micro-, meso- and macropore range (0.5 nm - 200 μm), density and active metal surface areas of various materials using many dedicated instruments for each application. The rate of product formation over a catalyst is a function of the accessible surface area of the active phase for materials not limited by mass transport of reactants to the active phase. Thus it is important to be able to quantify the surface area of this active phase, and the adsorption of inert gases makes this measurement possible (Thomas 1997). In spite of the oversimplification of the model on which the theory is

based, the Brunauer-Emmet-Teller (BET) method is the most widely used standard procedure for the determination of surface area of finely divided and porous material.

The BET method is based on a kinetic model of the adsorption process by Langmuir in which the surface of the solid was regarded as an array of adsorption sites. A dynamic equilibrium was assumed between the rate of molecules condensing from gas phase onto the bare sites and the rate at which molecules evaporate from occupied sites. The two rates are equal in equilibrium at that stage. The amount of gas adsorbed on a given adsorbent is measured as a function of the equilibrium partial pressure, p , of the adsorptive at constant temperature. The equilibrium partial pressure is preferably related to p_0 , the saturation vapor pressure of the adsorptive. Measurements are typically made at the temperature corresponding to the atmospheric boiling point of the adsorptive species (77 K for nitrogen). As mentioned, some simplified assumptions have been made; the famous BET equation applicable at low P/P_0 range is customarily written in linear form as:

$$\frac{p}{v_a(P - P_0)} = \frac{1}{V_m * C} + \frac{(C - 1)P}{V_m * C * P_0}$$

Where V^a is the number of moles adsorbed at the relative pressure P/P_0 , V_m is the monolayer capacity and C is the so-called BET constant which, according to the BET theory, is related to the enthalpy of adsorption in the first adsorbed layer and gives

information about the magnitude of adsorbent-adsorbate interaction energy (Rouquerol 1994).

If the information is applicable, a plot of $p/[V_a(P/P_o)]$ vs. P/P_o should yield a straight line with intercept $1/V_m C$ and slope $(C-1)/V_m C$. The value of V_m and C may then be obtained from a plot of a single line, or regression line, through the points (Webb P.A. 1997).

The volume of the monolayer ~~having been determined~~ allows the surface area of the sample to be determined by a single adsorbate molecule, a value derived from the assumption of close packing at the surface by the formula:

$$A_{BET} = V_m * a_m * L$$

where A_{BET} is the specific surface area, L is the Avogadro number and a_m is the molecular cross-sectional area of the gas molecule, which is assumed to be 0.162 nm^2 for nitrogen on an oxide surface (Ferdin 2002 a). The assumptions in the BET equation is no longer applicable if the BET plot is not linear, and the plot is usually restricted to the linear part of the isotherm over the p/p_0 range of 0.05-0.35 (Sing 1985).

The physisorption experiments are performed at very low temperature, usually at the boiling temperature of liquid nitrogen ~~at~~ atmospheric pressure. When a material is exposed to a gas, an attractive force acts between the exposed surface of the solid and the gas molecules. The result of these forces is characterized as physical (or Van der Waals) adsorption, in contrast to the stronger chemical attractions associated with chemisorption.

The surface area of a solid includes both the external surface and the internal surface of the pores. Due to the weak bonds involved between gas molecules and the surface (less than 15 KJ/mole), adsorption is a reversible phenomenon. Gas physisorption is considered non-selective, thus ~~filling the surface step by step (or layer by layer)~~ layering the surface, step by step dependings on the available solid surface and the relative pressure. Filling the first layer enables the measurement of the surface area of the material, because the amount of gas adsorbed when the mono-layer is saturated is proportional to the entire surface area of the sample. The complete adsorption/desorption analysis is called an adsorption isotherm. The six IUPAC standard adsorption isotherms [\(Figure 3.16\)](#) are shown below, they differ because the systems demonstrate different gas/solid interactions.

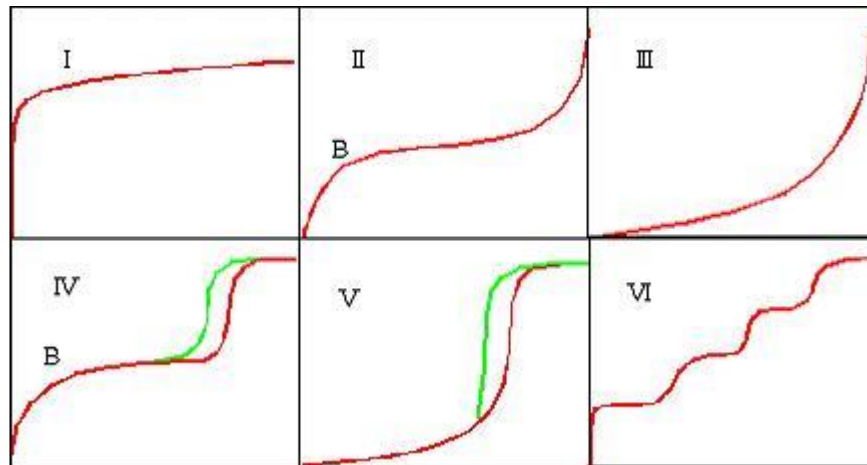


Figure 3.176: The IUPAC classification of adsorption isotherms

The Type I isotherm is typical of microporous solids and chemisorption isotherms. Type II is ~~shown~~ depicted by finely divided non-porous solids. Type III and type V are typical of vapor adsorption (i.e. water vapor on hydrophobic materials). Type VI and V feature a hysteresis loop generated by the capillary condensation of the adsorbate in the mesopores

of the solid. Finally, the rare type VI step-like isotherm is shown by nitrogen adsorbed on special carbon. Once the isotherm is obtained, a number of calculation models can be applied to different regions of the adsorption isotherm to evaluate the specific surface area (i.e. BET, Dubinin, Langmuir, etc.) or the micro and mesopore volume and size distributions (i.e. BJH, DH, H&K, S&F, etc.).

Pore dimensions cover a very wide range. Pores are classified according to three main groups depending on the access size:

- ◆ Micropores : less than 2 nm diameter
- ◆ Mesopores : between 2 to 50 nm diameter
- ◆ Macropores : larger than 50 nm diameter

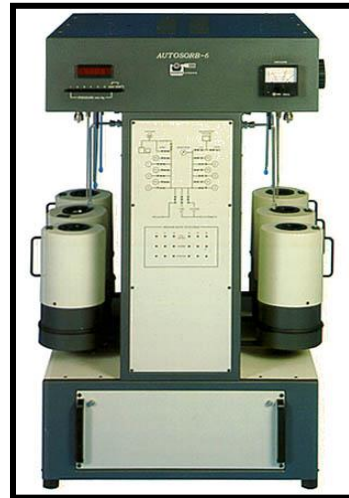


Figure 3.178: Quantachrome Autosorb Automated Gas Sorption System 6B

Principle of Operation

To investigate the porosity and surface area of the samples, the measurement was carried out ~~by using~~ Quantachrome Autosorb Automated Gas Sorption System 6B. About 2 g of sample was degassed at 393 K for 5 hours. Then, the total surface area of the catalyst was measured by Brunauer-Emmet-Teller (BET) method using nitrogen adsorption at 77 K. Adsorption of the injected gas onto the sample causes the pressure to slowly decrease until an equilibrium pressure is established in the manifold. The injection system consists of a calibrated piston, where both the pressure and the injection volume can be automatically varied by the system according to the adsorption rate and the required resolution. A small dead volume over the sample makes the instrument very sensitive to the amount of gas adsorbed. The equilibrium pressure is measured by a transducer chosen according to the pressure range where adsorption is established during the experiment.

The raw experimental data are the equilibrium pressures and the amount of gas adsorbed for each step. The gas uptake is calculated directly from the equilibrium pressure values but a dead volume calibration has to be performed before or after the measurement ~~by avia~~ “blank run” (that is an analysis using an inert gas not adsorbed on the sample in the analytical conditions, most commonly used is helium). The static volumetric method is very precise and is considered as a very accurate technique to evaluate surface area and pore size in the region of micro and mesopores. However it is not advisable whenever a

fast measurement of surface area is required, because this method involves long analysis time that are required to produce highly accurate and reliable results. The results were evaluated ~~with the~~using Autosorb Windows® for AS-3 and AS-6 Version 1.23.

3.7.5 Fourier Transform Infrared Spectroscopy

Infrared (IR) spectroscopy is one of the most common spectroscopic techniques used by organic and inorganic chemists. Simply, it is the absorption measurement of different IR frequencies by a sample positioned in the path of an IR beam. The main goal of IR spectroscopic analysis is to determine the chemical functional groups in the sample. Different functional groups absorb characteristic frequencies of IR radiation. Using various sampling accessories, IR spectrometers can accept a wide range of sample types such as gases, liquids, and solids. Thus, IR spectroscopy is an important and popular tool for structural elucidation and compound identification.

Infrared radiation spans a section of the electromagnetic spectrum having wavenumbers from roughly 13,000 to 10 cm^{-1} , or wavelengths from 0.78 to 1000 μm . It is bound by the red end of the visible region at high frequencies and the microwave region at low frequencies. IR absorption positions are generally presented as either wavenumbers (cm^{-1}) or wavelengths (λ). Wavenumber defines as the number of waves per unit length. Thus, wavenumbers are directly proportional to frequency, as well as the energy of the IR absorption. The wavenumber unit (cm^{-1} , reciprocal centimeter) is more commonly used in

modern IR instruments that are linear in the cm^{-1} scale. In ~~the~~ contrast, wavelengths are inversely proportional to frequencies and their associated energy.

Infrared spectroscopy (IR) is the study of the interaction of ~~the~~ infrared light with the sample. When infrared radiation is exposed, the sample could absorb lights, which corresponds to various energy ~~absorptions absorptions in it, causing large structures in transmittance and reflectivity spectra.~~ In far- IR region, free carrier dynamics and lattice vibration can be analyzed. In mid-IR region, chemical bonds can be detected, which could identify unknown functional groups contained in materials.



Figure 3.198: Fourier Transform Infra-Red Spectrophotometer

Principle of Operation

Fourier transform infrared transmission (FTIR) spectra were recorded with a Bruker spectrometer model IFS 66v/s, using the technique of KBr pellets and working with a

resolution of 4 cm^{-1} in the middle range. Before analysis, air evacuation was done under vacuum (5 mbar) for 15 minutes.

3.7.6 In-Situ Raman Spectroscopy

Raman Spectroscopy

is a spectroscopic technique used to observe vibrational, rotational, and other low-frequency modes in a system.^[1] It relies on inelastic scattering, or Raman scattering, of monochromatic light, usually from a laser in the visible, near infrared, or near ultraviolet range. The laser light interacts with molecular vibrations, phonons or other excitations in the system, resulting in the energy of the laser photons being shifted up or down. The shift in energy gives information about the vibrational modes in the system. Infrared spectroscopy yields similar, but complementary, information.

Typically, a sample is illuminated with a laser beam. Light from the illuminated spot is collected with a lens and sent through a monochromator. Wavelengths close to the laser line due to elastic Rayleigh scattering are filtered out while the rest of the collected light is dispersed onto a detector.

~~Raman Spectroscopy gives information about rotational and vibrational energy levels of a molecule, like IR spectroscopy.~~

Principle of Operation

Raman spectroscopy was performed on a Labram I (Dilor) instrument equipped with a confocal microscope (Olympus). A notch filter (Kaiser Optical) was applied to cut-off the

laser-line and the Rayleigh scattering up to 150 cm^{-1} . The spectrometer is equipped with a CCD camera (1024 × 298 diodes), which is Peltier cooled to 243 K to reduce the thermal noise. A HeNe laser (Melles Griot, 15 mW) was used to excite ~~the~~ Raman scattering at 632 nm. For the in situ solution experiments the laser beam was directed through the glass reaction vessel into the solution. The following spectrometer parameters were used: microscope objective, 10; slit width, 200 nm (spectral resolution, 2.5 cm^{-1}); integration time, 30 s per spectrum and 5 averages. For solution measurements, no power filter was applied. For powders, laser power was reduced to ca. 1 mW at the sample.

3.7.7 Thermal Analysis

Thermal analysis (TA) is frequently used to describe analytical experimental techniques which investigate the behavior of a sample as a function of temperature. The most widely distributed TA techniques are thermal gravimetry analysis (TGA), differential scanning calorimetry (DSC) and a differential thermal analysis (DTA). There are many other conventional techniques such as thermal mechanical analysis (TMA), dynamic mechanical analysis (DMA), alternating current calorimetry (ACC), and thermal luminiscence (TL).

TA is widely employed in both scientific and industrial domains. The ability of these techniques to characterize, quantitatively and qualitatively, a huge variety of materials over a considerable range has been crucial in their acceptance as analytical techniques.

The advantages of TA over other analytical methods can be summarized as follows:

- ◆ the sample can be studied over a wide temperature range using various temperature programmed
- ◆ almost any physical form of sample (solid, liquid or gel) can be accommodated using a variety of sample vessels or attachments
- ◆ a small amount of sample (0.1-10 g) is required
- ◆ the atmosphere in the vicinity of the sample can be standardized
- ◆ the time required to complete an experiment ranges from several minutes to hours
- ◆ TA instruments are reasonably priced

The recorded data are influenced by experimental parameters, such as the sample dimensions and mass, the heating/ cooling rate, the nature and composition of the atmosphere in the region of the sample and the thermal and mechanical history of the sample

(a) Thermal Gravimetric Analysis

Thermal Gravimetric Analysis (TGA) is the measure on the gain or loss in weight of a material as a function of the composition of the atmosphere and the temperature or of time. Further analysis of the weight loss steps requires the evaluation methods. As materials are heated, they can lose weight from a simple process such as drying, or from chemical reactions that liberate gasses. Some materials can gain weight by reacting with the atmosphere in the testing environment. Since weight loss and gain are disruptive processes to the sample material or batch, knowledge of the magnitude and temperature range of those reactions are necessary in order to design adequate thermal ramps and holds during those critical reaction periods.

It is a very useful technique for the study of solid-gas system and to characterize phase transformations. It also provides important quantitative information for the characterization of the thermal behavior of materials and investigates the influence of temperature and time on the formation of the sample. The quantitative determination of the component of interest in a mixture is often possible if it exhibits a single isolated weight loss.

The characteristics or properties can be measured by TGA such as drying, structural water release, structural decomposition, carbonate decomposition, gas evaluation, sulfur oxidation, fluoride oxidation and re-hydration. The measuring instrument is therefore a weighing device. ~~It has no memory that changes in the mass of the sample clearly imply evaluation or uptake of matter by sample. In weighing the sample it assumed that it can be connected to the weighing device.~~ The method only works well if the sample is in compact form.

TGA curves display **weight losses** that are typically caused by:

- Chemical reactions (decomposition and loss of water of crystallization, combustion, reduction of metal oxides)
- Physical transitions (vaporization, evaporation, sublimation, desorption, drying).

Occasionally a **gain in weight** is observed from:

- Chemical reactions (reaction with gaseous substances in the purge gas such as O₂, CO₂ with the formation of nonvolatile or hardlysemi volatile compounds)

• —

- — Physical transitions (adsorption of gaseous substances on samples such as active charcoal).

• —

• —



Figure 3.1919: Mettler Toledo TGA/SDTA851^e thermobalance

Principle of Operation

In principle, thermal stability of the catalyst can be measured by thermal gravimetric analyzer (TGA). The measurement was carried out using Mettler Toledo TGA/SDTA851^e thermobalance. 10-20 mg of catalyst was put into open alumina crucible of 100 μl that is supported on, or suspended from an analytical balance located outside the furnace chamber. The balance is zeroed, and the sample cup is heated according to a predetermined thermal cycle. The balance sends the weight signal to the computer for storage, along with the sample temperature and the elapsed time. The TGA temperature program was run dynamically from ambient to 548 K at a heating rate of 10 K min^{-1} under nitrogen gas with flow rate of 50 ml min^{-1} . Then, it was cooled to room temperature before being heated again under Argon gas from ambient to 873 K at a heating rate of 2 K min^{-1} with Argon gas at the same flow rate.

(b) Differential Scanning Calorimetric

Differential scanning calorimetry or **DSC** is a thermoanalytical technique in which the difference in the amount of heat required to increase the temperature of a sample and reference are measured as a function of temperature. Both the sample and reference are

maintained at very nearly the same temperature throughout the experiment. Generally, the temperature program for a DSC analysis is designed such that the sample holder temperature increases linearly as a function of time. The reference sample should have a well-defined heat capacity over the range of temperatures to be scanned. Therefore, the International Confederation for Thermal Analysis (ICTA) has defined DSC as a technique in which the difference in heat flow (or power) to the sample and to the reference material is monitored against time while the sample and reference material are subjected to a temperature program (Hemminger 1998). DSC therefore measures the amount of energy absorbed (endothermic event) or released (exothermic event) by a specimen either during continuous heating/cooling (dynamic or non-isothermal) experiments or during isothermal experiments (specimen maintained at a constant temperature). DSC can measure not only enthalpy changes, but also the rates of reaction, which lead, in principle, to kinetic parameter and to the reaction mechanisms (McNaughton 1975).

The basic principle underlying this technique is that, when the sample undergoes a physical transformation such as phase transitions, more (or less) heat will ~~need to flow to it than the reference pass through the sample~~ to maintain both the reference and sample at the same temperature. Whether more or less heat must flow to the sample depends on whether the process is exothermic or endothermic. For example, as a solid sample melts to a liquid it will require more heat ~~flowing passing through to~~ the sample to increase its temperature at the same rate as the reference. This is due to the absorption of heat by the sample as it undergoes the endothermic phase transition from solid to liquid. Likewise, as the sample undergoes exothermic processes (such as crystallization) less heat

is required to raise the sample temperature. By observing the difference in heat flow between the sample and reference, differential scanning calorimeters are able to measure the amount of heat absorbed or released during such transitions.

Differential scanning calorimetric can be used to measure a number of characteristic properties of a sample. The applications are numerous, either for routine quality control measurements, where automation capability and simple operation is required, or in research where high sensitivity and flexibility are important aspects. The DSC measurements are used for the following applications below:

- ◆ The oxidation stability
- ◆ Crystallinity of liquid samples
- ◆ Melting behavior
- ◆ Glass transition
- ◆ Kinetics
- ◆ Purity
- ◆ Specific Heat

DSC is widely used in the pharmaceutical, polymer industries, chemical ~~and food~~ and food science research as well.



Figure 3.200: METTLER TOLEDO DSC 822° equipment with an intra cooler

Principle of Operation

The differential scanning calorimetric analysis was performed using METTLER TOLEDO DSC 822° equipment with an intra cooler. The system was automated with a sample robot. About 10-50 mg of catalyst was placed into a hermetically sealed 40 µl Aluminium crucible, in a self-generated atmosphere with a pierced hole of approximately 50 µl. The temperature program was run dynamically from ambient to 823 K at heating rate of 5 K min⁻¹ under a constant nitrogen flow of 50 cm³ min⁻¹. The results were evaluated with the STAR^e software package.

(c) Temperature Programmed Reduction (TPR)

Temperature-programmed reduction (TPR) is a class of technique in which chemical reaction is monitored while the temperature increased linearly with time. These techniques are applicable to real catalysts and have the advantage of being experimental simple and

inexpensive in comparison to many other spectroscopy. Interpretation in a qualitative base is rather straight forward. Instrumentation for temperature programmed investigations is relatively simple (Nietmantsverdriet 2000).

The basic set up for TPR consists of a reactor and a thermal conductivity detector (TCD) to measure the hydrogen content in TPR of the gas mixture before and after reaction. More sophisticated TPR equipment consists of a mass spectrometer for the detection of reaction products. The area under a TPR curve represents the total hydrogen consumption and is commonly expressed in terms of moles of H_2 consumed per g of sample. TPR provides a quick characterization of metallic systems. This method gives information on the eventual degree of reduction of the phases present. For bimetallic catalysts, TPR pattern often indicate if the two components are mixed or not.



Figure 3.21: Temperature Programmed Desorption/Reduction/Oxidation (TPD/R/O)

Principle of Operation

TPR was carried out to determine the oxidation state and the chemical nature of metal species of the supported catalysts. Measurement was carried out in a Thermofinnigan TPDRO 1100 instrument. Then, approximately 100-300 mg of the catalyst was pre-treated in a tubular quartz reactor, by heating the material from room temperature to 303_K at 275_K min⁻¹ under 20_cm³ min⁻¹ N₂ for 20 minutes. This step is crucial in eliminating any possible contaminants present on the surface of catalyst. The material was cooled to room temperature again after pre-treatment. TPR measurement was carried out by flowing 20 cm³ min⁻¹ H₂ (5% H₂ in Nitrogen) from room temperature to 1273 K at a heating rate of 275_K min⁻¹ and hold isotherm, under flow of gas for 60 minutes. The reduction was measured by monitoring the hydrogen consumption with the TCD detector. The water produced during the reduction was trapped in a 5_Å molecular sieve column.

(d) Temperature Programmed Reaction Spectroscopy

Temperature Programmed Desorption (TPD), Temperature Programmed Reduction (TPR) and Temperature Programmed Oxidation (TPO) are the most commonly used tools for characterizing heterogeneous catalyst. These thermoanalytical techniques were used to

study the chemical interactions between gaseous reactants and solid substances (Kanervo 2003).

The most useful for single crystal and polycrystalline study is Temperature Programmed Desorption (TPD). When the technique is applied to a system in which the adsorption process is in part, irreversible and T-programming leads to surface reactions, then this technique is often known as Temperature Programmed Reaction Spectroscopy (TPRS). There is no substantive difference between TPRS and TPD. TPD also called Thermal Desorption Spectroscopy (TDS) where one studies desorption of gases from single crystal and polycrystalline foils into vacuum.

Temperature Programmed Reaction Spectroscopy (TPRS) is used to investigate the evolution of characteristic defects and catalytic performance in the bulk structure of MoVTeNb oxide catalyst under propene oxidation conditions. The basic experiment is involving, first, the adsorption of one or more molecular species onto the sample surface at low temperature (frequently 300K but sometimes sub-ambient). Second, heating of the sample in a controlled manner (preferably so as to give a linear temperature ramp) whilst monitoring the evolution of species from the surface back into the gas phase.



Figure 3.22: Temperature Programmed Reaction Spectroscopy

Principle of Operation

Temperature programmed reaction spectroscopy was performed by in-house fixed bed reactor equipped with the mass spectrometer. This reaction was done in Fritz Haber Institute. About 50 mg of sample was diluted with mixture of 50 mg of Boron Nitrate and 200 mg of Silicon Carbide into tubular micro reactor (refers on Figure 5.43.23). The reactor was heated by two thermocouples placed inside and outside the tube.

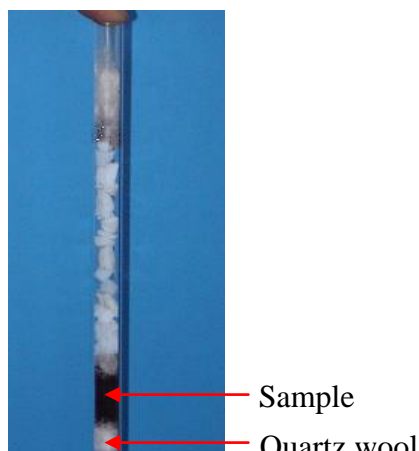


Figure 3.233: The tubular micro reactor filled with the catalyst

The reaction was carried by flowing 10 ml/min of propane, 10 ml/min of oxygen and 80 ml/min of helium. The total flow was 100 ml/min. The reactor was heated in two consecutive from room temperature to 773 K in constant feed with heating rate 5 ml/min and hold for 1h. The samples was cooled it down to 373 K for 30 min. The second reaction was heated from 373 K to 773 K with constant feed for another 80 min at heating rate 5 ml/min. The mass spectrometer is used to detect the products such as acrolein, propene, acrylic acid, acetic acid, carbon dioxide, carbon monoxide and other side products released form the reaction.

3.8 High-throughput Experimentation

The application of high-throughput experimentation including combinatorial methods for discovery of new heterogeneous catalysts is a fast developing area, which has attracted worldwide attention. Different high-throughput techniques for the preparation and the assessment of the catalytic performance of a large collection of samples have been developed. This development process is still continuing to meet the different needs of catalyst researches (Hanhndorf 2002).

The combinatorial approach requires at least three basic technologies. The first technology is the parallel synthesis of many promising candidates in a starting set of samples called “library”. The second technique is the evaluation candidates in a short time. The final technique is the optimization of successful candidates through design of a library of improved systems derived by exclusion from the previous library and by addition of new members or compositions (Yamada Y. 2001).

High-throughput experimentation is a suitable technique to accelerate the catalyst testing in early phases of development. In the strategy adopted for this research work, an attempt was made to use the catalytic data obtained under carefully controlled and validated conditions to derive at least semi-quantitative kinetic data and to map out a significant part of the parameter space that could be useful for more in-depth kinetic studies. In this way, the present work did not only concentrate on the selection of catalytic materials but rather used to derive a preliminary working hypothesis on the kinetic conditions of the target reaction. This hypothesis was used to develop an optimization strategy for the base catalyst. In contrast to the conventional optimization strategy, it was not the cationic chemical

composition that was varied but rather the unit operations of synthesis were modified to arrive at the most suitable nanostructuring the active phase. The high throughput testing was further used to derive a modification of the catalytic material called “dilution”. Chemically inert high-surface area diluents was introduced to achieve a separation of the active crystals with the active mass and so to avoid local hot spot formation in the highly exothermic selective oxidation.

Finally, the high throughput experimentation technique was also used to verify the testing conditions due to the effects of catalyst structure modifications (which will affect the chemical potential of the gas phase and hence, influencing the optimal point of operation in the environmental parameter space). This factor is usually not considered in screening campaigns that are operated under carefully controlled fixed conditions compared to screening campaigns with adaptive operating conditions. The present work will show that not only individual but group optimizations of the parameter space have substantial effects on the performance of a given system.

3.8.1 Highthroughput Nanoflow System

Currently, three general types of approaches have been utilized for the analysis of combinatorial libraries of heterogeneous catalyst (Caruthers 2003). The first approach is to implement currently available ‘one sample at a time’ techniques, such as mass spectrometry (MS) or gas chromatography, and combine them with multiple-well reactors and switching devices. These approaches are the easiest to implement with a small number of samples. It is, however, apparent that this method will consume too much time when large catalyst libraries are to be screened since the screening time is directly proportional to the number of samples to be analyzed.

The second analytical approach is based on the modification of conventional serial techniques using automation approaches in order to decrease the screening time. Amongst these are screening mass spectrometer (Krantz 2000; Rodemerck 2001; Ritcher 2002), gas chromatography (Hoffmann 2000; Reetz 2001), gas sensors (Yamada Y. 2001) and resonance-enhanced multiphoton ionization detection. All of these methods take advantage of the ability to run reaction in a parallel fashion but the testing is still performed in a sequential manner. At this stage, high-quality data are often sacrificed for improved speed by compromising the catalyst testing and therefore, make accurate evaluation of catalyst performance very difficult. The screening time is directly proportional to the number of samples to be analyzed.

The third approach involves truly parallel screening techniques, which gather data simultaneously from all catalysts in a library under realistic conditions. This category

includes infrared thermography, fluorescence imaging, and FTIR imaging. IR thermography has been used to detect activity for exothermic reactions in combinatorial libraries in a truly parallel fashion. However, thermal imaging does not possess any ability to chemically resolve product composition. Therefore, it is not clear whether any apparent activity observed is due to the desired reaction or unexpected side reactions. The techniques measure relative activity changes among a group of catalysts and is not truly quantitative (Su 2001; Caruthers 2003)

Each method above has its advantages and disadvantages. In terms of decreasing screening time and reproducibility the data, the second method, which is based on the modification of conventional serial techniques using automation approaches, is the best technique. This method takes advantage of the ability to run reactions in parallel fashion, but the testing is still performed in a sequential manner.



Figure 3.244: Highthroughput Nanoflow System

3.8 .2 Evaluation on Catalyst Screening and Catalytic Performance

3.8.2.1 Introduction on COMBICAT Nanoflow

COMBICAT Nanoflow catalytic reactor is one of the equipment that is used for this high throughput experimentation study (see Figure 3.25). This nanoflow catalytic reactor has multitubular reactors. It comprises of 12 quartz reactors connected to on-line gas chromatography realized in two parallel instruments to care for a complete analysis of the complex gas phase. The characteristics of this system is that the time for catalyst screening is decreased by factor of 12 compared to traditional test equipment (single continuous fixed-bed reactor), and that catalyst powder or small catalyst particles (size up to 200 micron) is exposed to gaseous reactant mixture which passes through the catalyst bed in plug-flow mode. This means that the catalyst screening can be carried out closely with under-nearly industrial process conditions.



Figure 3.25: The COMBICAT Nanoflow catalytic reactor system

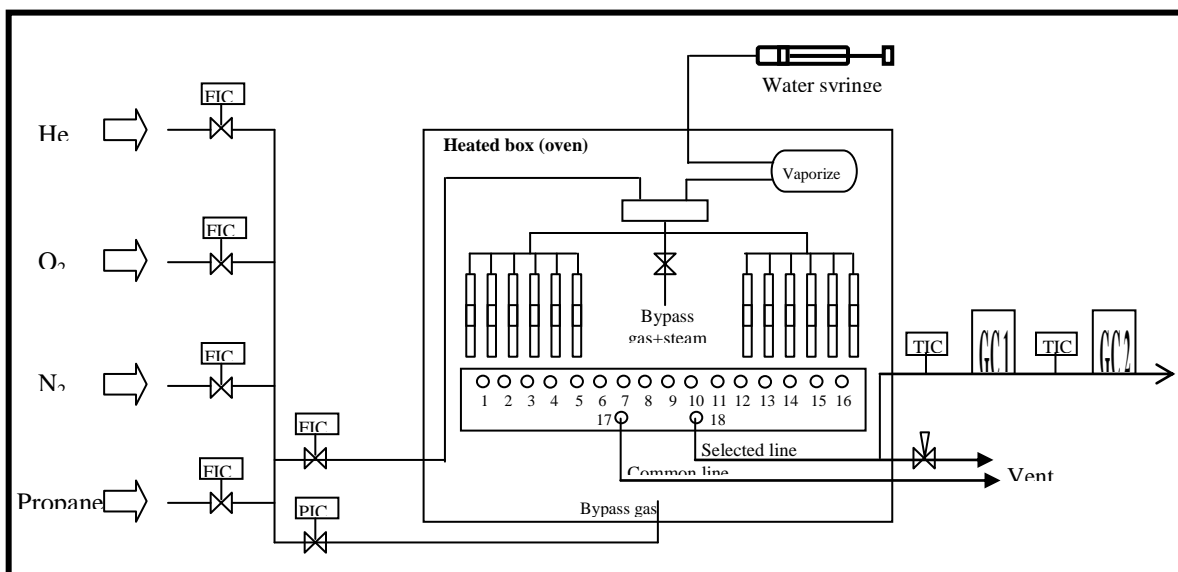


Figure 3.266: Process flow diagram of Combicat Nanoflow automated catalytic reactor system

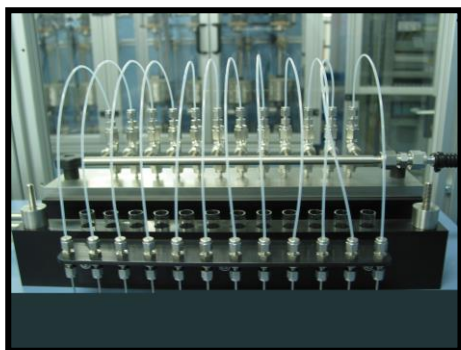


Figure 3.277: Reactor channel to the reactor blocks



Figure 3.288: Reactor tube



Figure 3.2929: Online GC Agilent HP6890N GC.

The schematic flow diagram of the high throughput experimenting system is shown in Figure 3.27. The set-up consists of two cubic ceramic banks with 6 reactors to each bank. Quartz tubes (i.d. = 4 mm, h = 220 mm), which are used as fixed-bed reactors, are concentrically arranged with respect to the axis of the bank. The catalyst bed is situated in the central part of the bank within the isothermal zone of the heating system.

The ends of all twelve-reactor channels are enclosed in a stainless steel cylinder sealed with chemical-resistant O-rings to avoid any gas leakage. The banks can be heated up to 873 K. To ensure isothermicity of the reaction zones in the center of the ceramic bank, heating is provided by an inner and an outer electrical heating element of rotational symmetry. Axial temperature profiles are controlled by thermocouples placed in each concentric ring of the reactor channels and it has been shown that the differences between temperatures in the 12 wells do not exceed 5 K. The gas flow through all reactor channels is controlled before and after each reactor by needle valves that need to be adjusted using a pre-set flow of an inert gas whenever the flow rate or the catalyst is to be changed.

For sampling, the reactor channel effluents are connected individually to a multi-port valves (1x18 port valves, heatable, Valco Instruments), which allow fast switching between the different reactor channels for sequential analysis of the reaction products without interruption of the gas flow. The pipes and switching elements are all mounted in a thermobox to avoid condensation, polymerization or thermal decomposition of products. The output liner to gas chromatography is also wrapped with heating tape to avoid deterioration of gas products.

The different feed gases streams are controlled by mass-flow controllers (Brooks Instrument). The liquid (water) feed is evaporated with a vaporizer set at 453 K. The mixing of steam and gases occurs in a gas-mixing chamber after the vaporizer to ensure the mixture is homogenous. The vaporizer, feeding lines and the mixer are installed inside the heated box to avoid condensation. The feed consisted of a mixture of propane, oxygen, nitrogen and water and introduced into the reactor block (Figure 3.27). By ascertaining close isothermicity and nearly equal flow rates in each reactor channel, the device is suitable for comparing the performance of different catalytic materials in each individual reactor tubes.

The COMBICAT Nanoflow catalytic reactor is set up to operate at pressures up to 1.5 barg and at temperatures up to 873 K. Each reactor channel can be filled with 300-600mg of catalytic material to obtain a catalyst bed volume of 0.5 ml (Figure 3.28). The catalyst is supplied as sieve fraction of pressed and crushed pellets from synthesized powder material. No shaping or forming aides were used for this study.

All reactor channels are remains on-stream during experimentation such that the activation or deactivation of the catalytic materials may be observed through multiple screening of the reactor channels under the same conditions as function of time on stream. A typical test run of a catalyst screening experiment is 120 h provided that the results are fairly significant for the catalyst stability tests with larger formulated active masses.

The compositions of all products were confirmed by two on-line gas chromatograph systems, GC (HP6890N, Agilent Technologies, Figure 3.29) with columns traps. Molecular sieve columns and Porapak columns with a thermal conductivity detector in first gas chromatographer were utilized for the analysis of inorganic gases and hydrocarbons (C₁-C₃). Capillary column (HP-FFAP) with a flame ionization detector in second gas chromatographer was utilized for the analysis of oxygenates hydrocarbons. The standard space velocity is equal to a GHSV of 1200 h⁻¹, and the standard volume catalytic bed of 0.5 ml. The standard feed composition is shown in Table 3.28.

Table 3.8: Feed gas ratio for 12 Nanoflow reactors

| Component | Normalized concentration | Concentration (vol%) |
|-----------|--------------------------|----------------------|
| Propane | 1 | 3.3 |
| Oxygen | 2.2 | 7.3 |
| Nitrogen | 17.8 | 59.3 |
| Steam | 9 | 30 |

3.8.2.2 Product Analysis

Usually in high-throughput screening of catalyst libraries, only the activity for a specific reaction by means of the degree of conversion or the heat reaction released is determined (Holzwarth 1999). Whilst for selectivity, frequently only the main products of interest are quantified (Weinberg 1998). The most common analysis techniques gas chromatography (GC) or mass spectrometry (MS) that are applied for product detection in the oxidative dehydrogenation or selective oxidation of light alkanes, show some drawbacks if used for

rapid detection in high-throughput experimentation. Gas chromatography allows a selective and sensitive detection of all products. The time for separation of all compounds ranging from 10-15 minutes for one analysis is generally considered to be too long. Complete analysis by MS is not possible due to the extensive superposition of fragment signals (Hanhndorf 2002). The analytics of the COMBICAT Nanoflow reactor is equipped with a dual gas chromatographic system for a fast and complete qualitative and quantitative analysis of the effluent gas using a combination of two fast GC (HP6890N, Agilent Technologies, and Figure 3.29) with columns traps. The abundance of all products was determined to close the carbon balance of the reaction. Values ~~of usually~~ above 98% for the carbon recovery were routinely obtained and the percentage of the carbon balance was used as internal quality control standard leading to interventions for values of below 95%.

Molecular sieve columns and Porapak columns with a thermal conductivity detector (TCD) in first gas chromatograph were utilized for the analysis of inorganic gases and hydrocarbons (C_1 - C_3). Haysep Q 80/100 traps hydrocarbon components, and permanent gases flow into a mole sieve column. After all hydrocarbon components flow into mole sieve column, the carrier gas transports all components inside mole sieve to the TCD detector and all components inside Haysep Q 80/100 to vent. Only the hydrocarbon fraction (C_1 - C_3) flows into HP-Plot Q then to TCD whilst the rest will be trapped into Haysep Q 80/100 ~~thenbefore~~ released to vent.

Capillary columns connected to a thermal conductivity detector (TCD) and to a flame ionization detector (FID) in the second gas chromatograph were utilized for analysis of hydrocarbons and oxygenated hydrocarbons. DB1 30m traps oxygenated hydrocarbon, and all hydrocarbon components flow into DB1 60m. After all hydrocarbon components flow into DB1 60m column, the carrier gas will transfer all components inside DB1 60m to TCD, and all components inside DB1 30m to vent. The fraction of oxygenated hydrocarbons flows into a DBFFAP column and then to FID whilst the rest will be trapped into HPFFAP then released to vent. Using the strategy of multi-column switching analysis, the COMBICAT Nanoflow reactor is able to perform a complete qualitative and quantitative analysis of the effluent gas of each reactor channel quickly. On average, the complete analysis of the gas chromatography time was reduced to 7 minutes (Widi 2004).